The Effect of Light-Induced Conical Intersection on the Photodissociation Dynamics of the D2(+) Molecule.

ARTICLE *in* THE JOURNAL OF PHYSICAL CHEMISTRY A · MARCH 2013

Impact Factor: 2.69 · DOI: 10.1021/jp401476q · Source: PubMed

4 AUTHORS, INCLUDING:

Ágnes vibók
University of Debrecen
103 PUBLICATIONS **1,116** CITATIONS
SEE PROFILE

Hans-Dieter Meyer
Universität Heidelberg
245 PUBLICATIONS **9,841** CITATIONS
SEE PROFILE

THE JOURNAL OF PHYSICAL CHEMISTRY A

Article

pubs.acs.org/JPCA

Effect of Light-Induced Conical Intersection on the Photodissociation Dynamics of the D_2^+ Molecule

Gábor J. Halász[†,§] and Ágnes Vibók*[,‡,§]

[†]Department of Information Technology, University of Debrecen, H-4010 Debrecen, P.O. Box 12, Hungary

[‡]Department of Theoretical Physics, University of Debrecen, H-4010 Debrecen, P.O. Box 5, Hungary

Hans-Dieter Meyer[§] and Lorenz S. Cederbaum[§]

[§]Theoretische Chemie, Physikalish-Chemisches Institut, Universität Heidelberg, H-69120 Heidelberg, Germany

ABSTRACT: It is known that conical intersections (CIs) can be induced by laser light even in diatomics. In the close vicinity of these laser-induced CIs (LICIs) the nonadiabatic effects are infinitely strong, as is the case for naturally appearing CIs in field-free polyatomics. In the present work we study the photodissociation dynamics of the D_2^+ molecule in an intense laser field to investigate the role of the LICI. Specifically, the kinetic energy release (KER) and the angular distribution of the photodissociation products are calculated with and without LICI for different initial conditions and for different values of the laser parameters. To do so, both one- and two-dimensional calculations were performed. In the first model the molecules were rotationally frozen, whereas in the latter one, the molecular rotation is included as a full additional dynamic variable. The results obtained undoubtedly demonstrate the strong impact of the coupling of the rotation to the vibrational and electronic motions and hence of the LICI on the dissociation dynamics of the D_2^+ molecule.

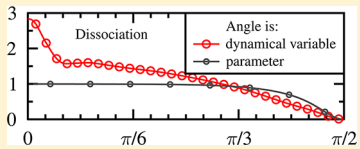

I. INTRODUCTION

Nonadiabatic processes are ubiquitous in photophysics and photochemistry. It has been demonstrated for a large variety of examples that conical intersections (CIs) between electronic potential energy surfaces provide a mechanism for extremely fast chemical processes, e.g., photodissociation, photoisomerization, and internal conversion to the electronic ground state. The CIs are thus considered as photochemically relevant decay channels. CIs can be appear for different electronic states starting ranging from triatomic systems to truly large polyatomic molecules. Several important books, review articles, and publications have demonstrated the existence and relevance of such intersections in recent decades.[1−6]

CIs in molecules can be formed only if the studied molecular system possesses at least two independent nuclear degrees of freedom. Therefore, having only one nuclear vibrational coordinate, CIs cannot appear for a diatomic molecule. However, this latter statement is true only in free space. The electronic energy of diatomics exposed to strong laser fields depends on the angle between the polarization of the field and the molecular axis because the interaction of the induced or permanent dipole moment of the system with the electric field leads to an effective torque toward the polarization direction. It was presented in earlier works[7,8] that CIs can be formed by both running and standing laser waves even in diatomics. In these situations, additional to the nuclear vibration, the rotational (or the center of mass) motion provides the missing degree of freedom to make possible the formation of a light-induced conical intersection (LICI) that introduces strong nonadiabatic couplings via mixing the rotational, vibrational, and electronic motions. This process in running waves and laser pulses is easily understood within the framework of the dressed state representation. Describing the laser−matter interaction in this model, in which the laser field is explicitly included in the Hamiltonian, the change of the electronic energies leads to the appearance of the LICI. The energetic and spatial positions of the light-induced CI can be controlled by varying the parameter settings (intensity, frequency) of the laser field. Detailed theoretical investigations demonstrate that these light-induced CIs can have severe impact on the dynamical properties of the molecule.[9,10−12] We note that in a very recent publication the LICI has also been studied for polyatomics by Martinez, Bucksbaum, and their co-workers.[13]

In the present study the impact of the LICI on the photodissociation dynamics of the D_2^+ molecule is discussed. The kinetic energy release (KER) spectra and the angular distribution of the photodissociation products are calculated with and without LICIs for different initial conditions and for several different values of the laser parameters. By solving the time-dependent nuclear Schrödinger equation (TDSE), we have performed both two (2D) and one (1D) dimensional calculations. More precisely, the molecular rotational angle is fully included in the numerical simulations as a dynamic variable in the 2D calculations, and is only a parameter in the

Special Issue: Structure and Dynamics: ESDMC, IACS-2013

Received: February 10, 2013
Revised: March 27, 2013
Published: March 27, 2013

   dx.doi.org/10.1021/jp401476q | J. Phys. Chem. A 2013, 117, 8528−8535

1D computations. It is expected that taking into account the rotation explicitly in the description of the photodissociation of the D_2^+, the results obtained are sensitive to the initial orientational distribution of the molecules. This issue will also be discussed in detail. Finally, we note here that several important works were recently published to stress the importance of the role of molecular rotation[18,27,28] in the correct description of molecular photodissociation.

This paper is structured as follows. In section II, the applied methods and the calculated quantities are briefly reviewed. In section III, we present and analyze the numerical results for several different initial conditions and laser parameters. Conclusions are provided in section IV.

II. METHODOLOGY

Let us consider the D_2^+ ion as our sample system. Although it is a very simple molecule and numerous theoretical and experimental studies have been performed on it in strong laser field,[14−38] there are still unclarified issues. In addition, due to its relative simplicity, one can study light-induced nonadiabatic phenomena separately from other processes. In our model calculations we will consider the ground state of the D_2 molecule ($X^1\Sigma_g^+$) and the two relevant electronic states of the D_2^+ ion, which are characterized by the $V_1 = 1s\sigma_g$ and $V_2 = 2p\sigma_u$ potential energy curves, respectively. To study the dissociation process, the following two-step mechanism will be considered (Figure 1): (i) At first the molecule in its ground ($X^1\Sigma_g^+$) state is ionized and a vibrational wave packet is launched to the $1s\sigma_g$ state of D_2^+ in the Franck−Condon region. (ii) As a second step, the D_2^+ ion is excited from the $1s\sigma_g$ state by a laser pulse to the repulsive $2p\sigma_u$ state. Due to the electric field of the laser the $1s\sigma_g$ and $2p\sigma_u$ electronic states are coupled. The nonvanishing dipole matrix elements are responsible for the light-induced electronic transitions. In the space of these two electronic states the following time-dependent Hamiltonian holds for the rovibronic nuclear motions:

$$H = \begin{pmatrix} -\frac{1}{2\mu}\frac{\partial^2}{\partial R^2} + \frac{L_{\theta\varphi}^{\ 2}}{2\mu R^2} & 0 \\ 0 & -\frac{1}{2\mu}\frac{\partial^2}{\partial R^2} + \frac{L_{\theta\varphi}^{\ 2}}{2\mu R^2} \end{pmatrix} + \begin{pmatrix} V_1(R) & -\varepsilon_0 f(t)\, d(R) \cos\theta \cos\omega_L t \\ -\varepsilon_0 f(t)\, d(R) \cos\theta \cos\omega_L t & V_2(R) \end{pmatrix} \quad (1)$$

Here, R and (θ, φ) are the molecular vibrational and rotational coordinates, respectively, μ is the reduced mass, and $L_{\theta\varphi}$ denotes the angular momentum operator of the nuclei. Here θ denotes the angle between the polarization direction and the direction of the transition dipole and thus one of the angles of rotation of the molecule. $V_1(R)$ ($1s\sigma_g$) and $V_2(R)$ ($2p\sigma_u$) are the field-free potential curves of the two electronic states coupled by the laser (whose frequency is ω_L and maximal amplitude is ε_0), $f(t)$ is the envelop function, and $d(R)$ ($=-\langle\psi_1^e|\sum_j r_j|\psi_2^e\rangle$) is the transition dipole matrix element ($e = m_e = \hbar = 1$ atomic units are used throughout the article). The potential energies $V_1(R)$ and $V_2(R)$ and the transition dipole moment were taken from.[39,40]

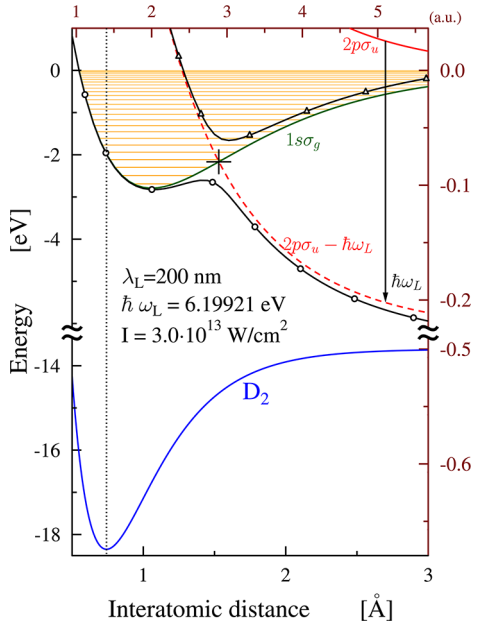

Figure 1. Potential energy curves. Shown are the curves for the ground state ($X^1\Sigma_g^+$) of D_2, and for the ground ($1s\sigma_g$), first excited ($2p\sigma_u$), and field dressed ($2p\sigma_u - \hbar\omega$) states of the D_2^+ ion. The first laser pulse ionizes the D_2 molecule to create a vibrational wave packet on the $1s\sigma_g$ surface of D_2^+. The solid green and red lines show the field-free energies of the ground and first excited states of the ion, respectively, which are the diabatic energies when the field is on. The energy of the field dressed excited state ($2p\sigma_u - \hbar\omega_L$; dashed red line) crosses the energy of the ionic ground state at the point where the light induced conical intersection (LICI) of these two states is formed. These curves can also be viewed as cuts through the adiabatic surfaces at $\theta = \pi/2$ where the interaction between the states via the field vanishes. For further visualization, cuts of the adiabatic surfaces at $\theta = 0$ (parallel to the field polarization) are shown for a field intensity of 1×10^{14} W/cm^2. The cuts through the lower and upper adiabatic surfaces are depicted by solid black lines marked with circles and triangles, respectively. The position of the LICI (R_{LICI} = 1.53 Å = 2.891 au and E_{LICI} = −2.16611 eV) is marked with a cross.

It is known that the dressed state representation is very illustrative and helps to understand the essence of the light-induced nonadiabatic effects. In this representation the laser light shifts the energy of the $2p\sigma_u$ repulsive excited potential curve by $\hbar\omega_L$ and a crossing between the diabatic ground and the diabatic shifted excited potential energy curves is formed. After diagonalizing the potential energy matrix, one can obtain the adiabatic potential surfaces V_{lower} and V_{upper} (Figure 1). These two surfaces can cross each other, giving rise to a conical intersection whenever these two conditions $\cos\theta = 0$ ($\theta = \pi/2$) and $V_1(R) = V_2(R) - \hbar\omega_L$ are simultaneously fulfilled.

The characteristic features of the LICI can be changed by varying the frequency and intensity of the laser field. Increasing the frequency, for example, moves the CI to a smaller internuclear distance and to a smaller energetic position. The steepness of the CI cone formed by the adiabatic surfaces, which is related to the strength of the nonadiabatic coupling,[1−5] can be controlled by the laser intensity.

To take account of the impact of the LICI on the photodissociation dynamics, one has to solve the time-dependent nuclear Schrödinger equation (TDSE) with the Hamiltonian $\hat{H}$ is given by eq 1. One of the most efficient approaches for solving the time-dependent nuclear Schrödinger equation is the MCTDH (multiconfiguration time-dependent

dx.doi.org/10.1021/jp401476q | J. Phys. Chem. A 2013, 117, 8528−8535

Hartree) method.[41−45] To describe the vibrational degree of freedom, we have used FFT-DVR (fast fourier transformation-discrete variable representation) with N_R basis elements distributed on the range from 0.1 au to 80 au for the internuclear separation. The rotational degree of freedom was described by the Legendre polynomials $\{P_J(\cos\theta)\}_{j=0,1,2,...,N_\theta}$. These so-called primitive basis sets (χ) were used to represent the single particle functions (ϕ) which in turn were used to represent the wave function:

$$\phi_{j_q}^{(q)}(q,t) = \sum_{l=1}^{N_q} c_{j_q l}^{(q)}(t)\,\chi_l^{(q)}(q) \qquad q = R, \theta \tag{2}$$

$$\psi(R,\theta,t) = \sum_{j_R=1}^{n_R}\sum_{j_\theta=1}^{n_\theta} A_{j_R,j_\theta}(t)\,\phi_{j_R}^{(R)}(R,t)\,\phi_{j_\theta}^{(\theta)}(\theta,t)$$

In our numerical calculations we have used N_R = 2048 and, depending on the field intensity, N_θ = 6, ..., 70. On both diabatic surfaces and for both degrees of freedom a set of n_R = n_θ = 3, ..., 25 single particle functions were used to build up the nuclear wave function of the system. (The actual value of N_θ and n_R = n_θ was chosen depending on the peak field intensity I_0.) All the calculations were correctly converged with these parameters. Due to the cylindrical symmetry of the problem, L_φ = m is a good quantum number and we have concentrated on discussing the m = 0 case exclusively.

Using the nuclear wave function, we calculated the kinetic energy release (KER) and the angular distribution of the photofragments:[43]

$$P_{\mathrm{ker}}(E) = \int_0^\infty \mathrm{d}t \int_0^\infty \mathrm{d}t'\,\langle\psi(t)|W|\psi(t')\rangle \mathrm{e}^{-\mathrm{i}E(t-t')} \tag{3}$$

where $-\mathrm{i}W$ is the complex absorbing potential (CAP) applied at the last 5 au of the grid related to the vibrational degree of freedom ($W = 0.00005\cdot(r-70)^3$, if $r > 70$ au on the $1s\sigma_g$ surface and $W = 0.00236\cdot(r-75)^3$, if $r > 75$ au on the $2p\sigma_u$ surface), and

$$P(\theta_j) = \frac{1}{w_j}\int_0^\infty \mathrm{d}t\,\langle\psi(t)|W_{\theta_j}|\psi(t)\rangle \tag{4}$$

where $-\mathrm{i}W_{\theta_j}$ is the projection of the CAP to a specific direction of the angular grid (j = 0, ..., N_θ), and w_j is the weight related to this grid point according to the applied DVR.

To demonstrate the impact of the rotation on the dissociation process of D_2^+, we compare the results obtained from the full two-dimensional calculations (2D) with those obtained for a one-dimensional model (1D). In the first case the rotation is included in the numerical calculations (i.e., the rotational coordinate is a dynamical variable), whereas in the second situation the rotation is frozen as the rotational coordinate is treated as a parameter. Under this condition the initial orientation of the molecules is fixed during the dissociation process and the "effective field strength" in the Hamiltonian eq 1 is given by the projection of the field on the axis of the molecule: $\varepsilon_0^{\mathrm{eff}} = \varepsilon_0\cdot\cos\theta$ ($I_0^{\mathrm{eff}} = I_0\cdot\cos^2\theta$). This restriction implies that the molecular rotation is frozen and therefore the orientation of the molecular axis relative to the polarization of the laser field does not change during the whole process.

III. RESULTS AND DISCUSSION

In the numerical simulation linearly polarized Gaussian laser pulses centered around t = 12.3 fs were used. It is the time when the mean of the internuclear distance of the ground state wavepacket vertically transferred to the ground state of the ion reaches its maximal value in the field-free case. The center wavelength is 200 nm and the pulse duration defined by its full width at half-maximum (fwhm) is 30 fs. Several different intensity values have been employed ranging between 1×10^{11} and 3×10^{14} W/cm^2.

The vibrational ground state of the neutral molecule transferred vertically to the potential energy curve of the ground electronic state of the ion served at the initial wave packet. This Franck−Condon distribution of the vibrational states of the ion has been used. The initial wave packet can be viewed as the superposition of all the vibrational states of D_2^+ needed to reproduce the vibrational ground state of the neutral D_2.

A. Discussion of the Alignment. As is well-known, the initial alignment of the molecules has a strong effect on the angular distributions of the photofragments.[25] To study this effect in the presence of molecular rotations, different initial alignments were considered in the calculations. We assumed molecules initially in an unaligned (i.e., isotropic) distribution, as well as in preliminary aligned (parallel and perpendicular) initial distributions. For the isotropic distribution the nuclear wave packet was initially in its rotational ground state (J = 0).

Leaving alone the prealigned (either parallel or perpendicular) molecules, the preferred direction disappears after a while even without the presence of an external electric field because the molecules start rotating toward the isotropic arrangement. This isotropic arrangement is reached after a long time, but the rotation into this direction could be observed even in the first few femtosecons. If the electric field is present, it turns the molecules toward the parallel arrangement where the potential is deepest. If the initial arrangement is perpendicular to the polarization direction, these two effects reinforce each other. But, if the initial arrangement is parallel to the polarization direction, then these two effects work against each other and it depends on the intensity of the field and the pulse duration which effect will have a stronger impact on the molecular orientation. In our examples we see that the rotation toward the parallel arrangement dominates only at the range of the largest intensities used. To demonstrate these effects, we assumed isotropic, parallel, and perpendicular initial arrangements of the molecules and made snapshots of the angular distribution of the wave packet at times t = 0 and t = 12.3 fs. The results are displayed in Figure 2.

B. Kinetic Energy Release (KER). The results obtained for the KER spectra (eq 3) are illustrated in Figures 3−6. In the numerical simulations we assumed initially aligned (parallel and perpendicular to the electric field) as well as unaligned (isotropic) molecules. Several different intensities from 1×10^{11} to 3×10^{14} W/cm^2 were applied.

By studying Figure 3, we find that the first conspicuous result is that for the case of parallel initial orientation regardless of the applied intensity the 1D and 2D calculations are practically the same. This is not surprising because there is no rotation for this initial orientation (see also the discussion of the alignment above). This is not true, however, for the other two initial arrangements. In these cases there are significant differences between the two models and this effect is more pronounced for

dx.doi.org/10.1021/jp401476q | J. Phys. Chem. A 2013, 117, 8528−8535

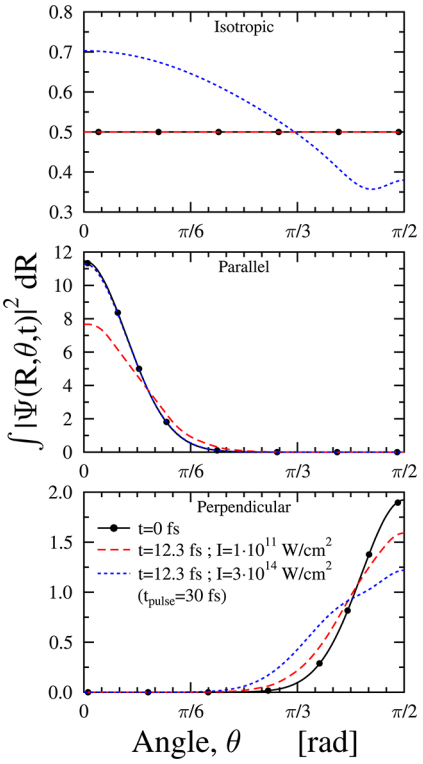

Figure 2. Alignment of the D_2^+ ions at the time t = 12.3 fs for different initial alignments at t = 0. Shown are the results for isotropic, parallel, and perpendicular initial alignments. Two different intensities 1×10^{11} and 1×10^{14} W/cm^2 are applied.

higher intensities (Figure 4). These findings are expected, because the rotation has a very significant role for these geometrical arrangements. The dissociation probability is strongly dependent on the initial alignment of the molecules. In the parallel initial orientation the molecules can dissociate easily even at low intensities. The dissociation probability is then the largest one when compared with the other two arrangements. However, the shape of the spectra clearly shows that they do not dissociate immediately at low intensities. The interference pattern of the spectra appears as a consequence of the finding that the different parts of the wave packet dissociate after a different number of oscillations in the potential valley (Figure 3a). In the 1D case this can happen if the effective field intensity is moderate; otherwise, the wave packet dissociates in a single step. This situation is encountered at the highest intensities only at the vicinity of the perpendicular orientation. Therefore, the 1D curves display interferences only when the initial orientation includes this region. At larger intensities "the structure" disappears from the spectra (Figure 3b) because the parallel aligned molecules can dissociate almost immediately. Their spectra are smooth regardless of whether they were obtained by using the 1D or 2D model. On the other hand, the rich pattern of the two other spectra for the perpendicular and isotropic initial arrangements does not vanish even for high intensities. Under such conditions the molecules are not able to dissociate immediately.

For larger intensities the pattern is more pronounced in the spectra of the initially perpendicular molecules than in the isotropic spectra because among the latter initially parallel molecules are also included. These do not contribute to the additional structures as they dissociate immediately.

It is worth noting that below the intensity of 1×10^{13} W/cm^2 the dissociation probability of the vibrational level $\nu = 5$ is practically zero (Figure 5). Fragment energies from the $\nu = 5$ vibrational eigenstate of the ion in its electronic ground state are missing in the spectra. To understand and to explain these interesting properties more deeply requires the analysis of the photofragments from single vibrational levels. This will be subject of future investigations.

For low intensities the maximum values of the energy distribution of the dissociating particles almost perfectly coincide with the shifted energies of the vibrational levels of the ground electronic states of D_2^+ (Figure 6a). When the intensities increase, this feature changes definitely. The positions of the peeks in the 2D calculations for the initially perpendicular and also for the isotropic arrangements are clearly shifted (Figure 6b). As the intensity is increased, at first the low energy range displays this shifting (Figure 4) and as the intensity is increased further also the higher energy range is affected (Figure 6b). The shifts of the photofragment energies are substantial and can be explained as follows. Due to the significant rotation induced by the electric field, rotational energies additionally contribute to the kinetic energy of the outgoing photofragments. In addition, there is another effect. With the growing of the light intensity the lower adiabatic potential well becomes wider and the energetic spacing between the vibrational levels decreases. This is also a typical two-mode interaction effect that is fully accounted for by the 2D calculations. The sum of these two effects can cause the observed energy shift in the spectra. This strongly contrasts the 1D spectra. Here, the maxima of the computed peaks remain at

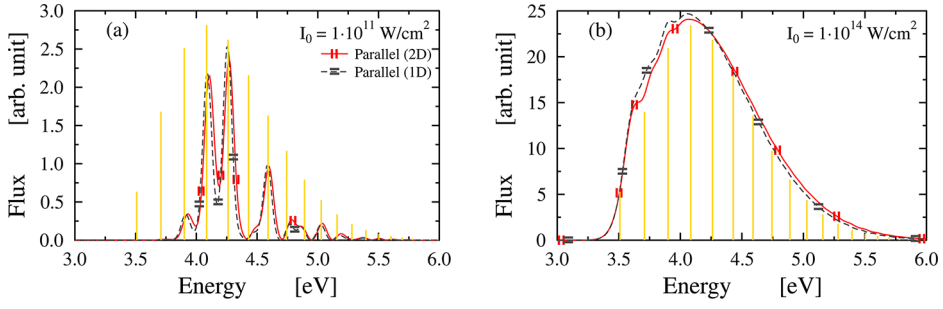

Figure 3. Kinetic energy release (KER) spectra of the D_2^+ photofragments for parallel initial orientations at 1×10^{11} and 1×10^{14} W/cm^2 intensities. The 1D and 2D curves correspond to the one-dimensional (no LICI situation) and the two-dimensional calculations, respectively. Vertical lines denote the different vibrational levels of the D_2^+ molecule in the field-free case shifted by the photon energy ($\hbar\omega_L$). The height of these lines is proportional to the population of the vibrational levels in the initial wave packet (Franck–Condon principle).

dx.doi.org/10.1021/jp401476q | J. Phys. Chem. A 2013, 117, 8528–8535

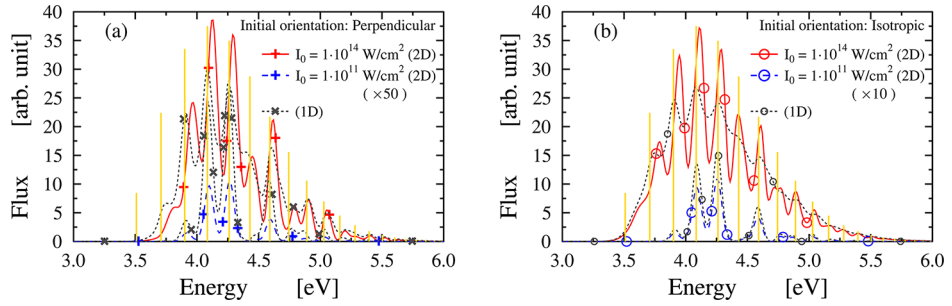

Figure 4. Kinetic energy release (KER) spectra of the D_2^+ photofragments for perpendicular initial orientations at 1×10^{11} and 1×10^{14} W/cm^2 intensities (a). Kinetic energy release (KER) spectra of the D_2^+ photofragments for isotropic initial distribution at 1×10^{11} and 1×10^{14} W/cm^2 intensities (b). For more details, see Figure 3.

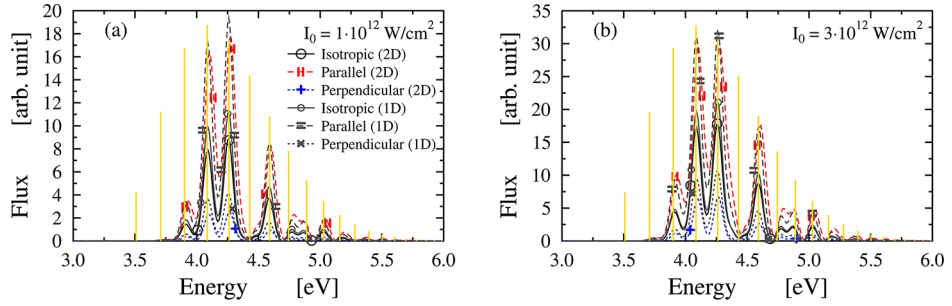

Figure 5. Kinetic energy release (KER) spectra of the D_2^+ photofragments for perpendicular, parallel, and isotropic initial alignments at 1×10^{12} and 3×10^{12} W/cm^2 intensities. For more details, see Figure 3.

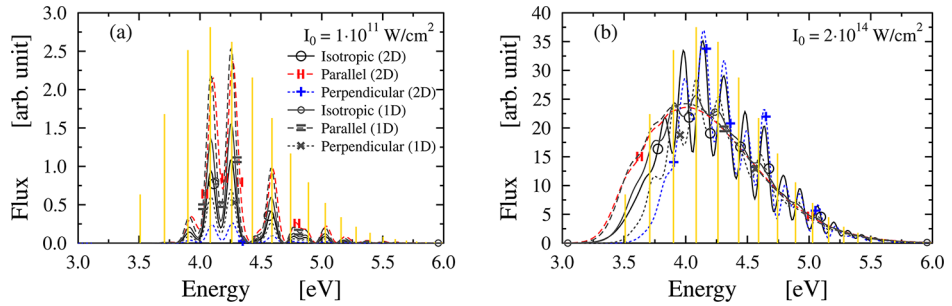

Figure 6. Kinetic energy release (KER) spectra of the D_2^+ photofragments for perpendicular, parallel, and isotropic initial alignments at 1×10^{11} and 2×10^{14} W/cm^2 intensities. For more details, see Figure 3.

the positions of the field-free vibrational levels because this model does not account the molecular rotation and certainly not for the LICI.

C. Angular Distribution. The results of the computations of the angular distributions of the photofragments (eq 4) are presented in Figures 7 and 8. It is eye-catching that for larger intensities the full 2D distributions for both the initially isotropic and perpendicular orientations exhibit a characteristic humped structure, whereas in the respective 1D calculations these additional patters cannot be seen (Figure 7 panels c and d). In section A we have already discussed the role of the rotation in the description of the dynamical behavior of molecules for both the initial isotropic and perpendicular orientations. The inclusion of the molecular rotation in the 2D model implies the formation of a LICI in the D_2^+ molecule, and this should contribute and might even be the reason of the bumpy structure on the angular distribution curves. The LICI introduces an intense nonadiabatic coupling and strongly mixes the rotational and vibrational motions on both electronic surfaces, and therefore, even if one starts with a $J = 0$ state, we do afterward find J values up to 30 or even 40! In accordance with the increasing J values, more and more rotational nodes are forming, giving rise to the bump structure in the angular distribution curves. In accordance with this explanation, these humps are always missing in the curves obtained for the initially parallel aligned molecules, as there is only minor rotation involved in this situation (Figure 7 panels a and b). We note here that this effect is more pronounced with increasing intensity.

There is another interesting observation. The 1D and 2D angular distributions can be quite different even at lower intensity. This applies to results for the initially parallel and perpendicular aligned molecules whereas for the isotropic arrangement they nicely agree. This behavior is clearly visible on the zoomed version of the picture (Figure 8). It is due to the fact that the system starts rotating; however, rotations are not taken into consideration in the 1D model. For the isotropic initial arrangement there is no such kind of "self-orientation" toward the isotropic arrangement as the system is inherently isotropic. For stronger intensities a completely different situation applies. Here, the 1D and 2D curves are very close to each other only in the parallel case, but the angular

dx.doi.org/10.1021/jp401476q | J. Phys. Chem. A 2013, 117, 8528−8535

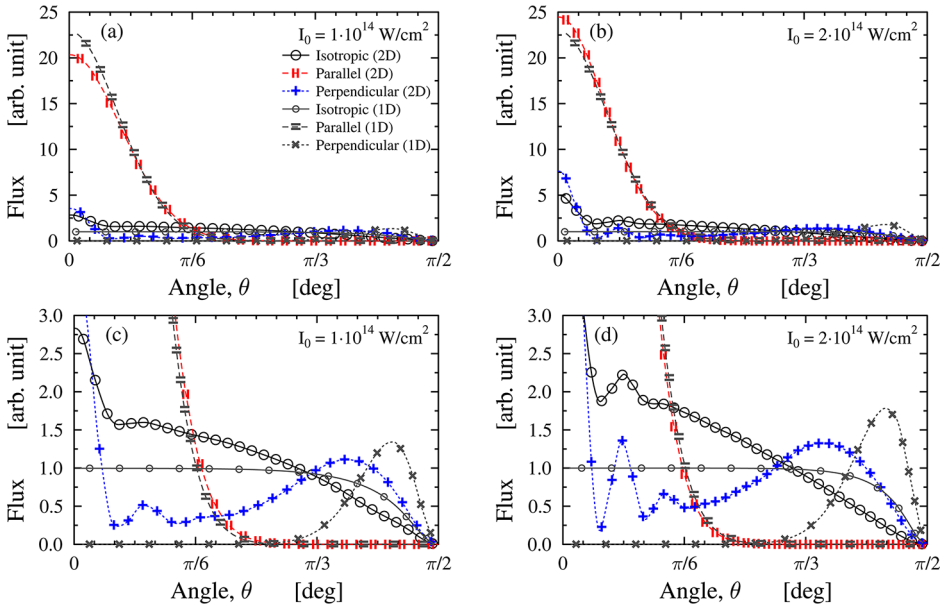

Figure 7. Angular distributions of the D_2^+ photofragments for perpendicular, parallel, and isotropic initial alignments at 1×10^{14} and 2×10^{14} W/cm^2 intensities. The curves denoted 1D and 2D correspond to the one-dimensional (no LICI situation) and to the two-dimensional calculations, respectively.

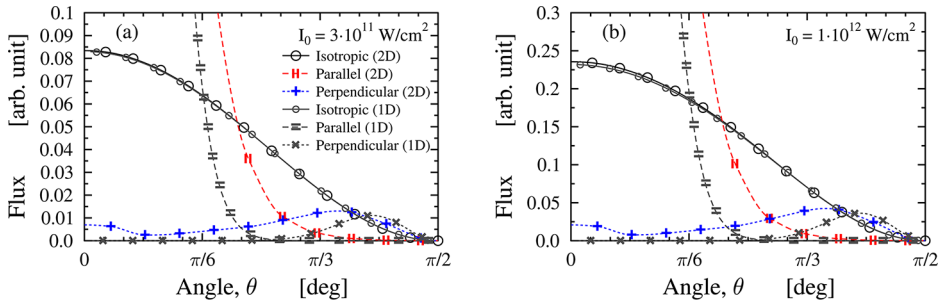

Figure 8. Angular distributions of the D_2^+ photofragments for perpendicular, parallel, and isotropic initial alignments at 3×10^{13} and 1×10^{12} W/cm^2 intensities. The curves denoted 1D and 2D correspond to the one-dimensional (no LICI situation) and to the two-dimensional calculations, respectively.

distribution functions are very different in the other two cases (Figure 7 panels c and d). The mechanism is as follows. In the parallel case the 1D and 2D results are very similar because the high field intensity is able to hold together the initially parallel oriented molecules. The field applied is strong enough to keep the orientation aligned parallel without broadening the initial distribution. In the isotropic and perpendicular cases the molecules can rotate in the high intensity electric field and this destroys the initial orientations. This demolition of the initial alignment cannot be accounted for in the 1D model, however, and therefore, at higher intensities the 1D and 2D results strongly differ from each other.

IV. CONCLUSIONS

In summary, we have performed one- and two-dimensional calculations of the photodissociation process of D_2^+ in an intense laser field. In the one-dimensional simulations only the nuclear vibrational degree of freedom is taken into account in the dynamics and the rotational angle is just an external parameter. The two-dimensional fully quantum mechanical calculations contain the molecular rotations as well as the nonadiabatic coupling between the rotations, vibrations, and electronic motion. A particularly appealing feature of taking properly into account the dynamic interplay of all motions is the formation of light induced conical intersections which can give rise to severe nonadiabatic effects similar to the situation in polyatomics, where conical intersections appear naturally in field-free space.

AUTHOR INFORMATION

Notes

The authors declare no competing financial interest.

ACKNOWLEDGMENTS

The authors acknowledge the financial support by the Deutsche Forschungsgemeinschaft (Project ID CE10/50-1). Á.V. acknowledges the OTKA Grant no. NN103251. The publication was supported by the TÁMOP-4.2.2.C-11/1/KONV-2012-0001 project. The project has been supported by the European Union, cofinanced by the European Social Fund.

REFERENCES

(1) Köppel, H.; Domcke, W.; Cederbaum, L. S. Multimode Molecular Dynamics beyond the Born-Oppenheimer Approximation. *Adv. Chem. Phys.* **1984**, *57*, 59−246.

(2) Baer, M. Introduction to the Theory of Electronic non-adiabatic Coupling Terms in Molecular Systems. *Phys. Rep.* **2002**, *358*, 75−142.
(3) Worth, G. A.; Cederbaum, L. S. Beyond Born-Oppenheimer: Molecular Dynamics through a Conical Intersection. *Annu. Rev. Phys. Chem.* **2004**, *55*, 127−158.
(4) Domcke, W., Yarkony, D. R. and Köppel, H. *Conical Intersections: Electronic Structure, Dynamics and Spectroscopy*; World Scientific: Singapore, 2004.
(5) Baer, M. *Beyond Born Oppenheimer: Electronic Non-Adiabatic Coupling Terms and Conical Intersections*; Wiley: New York, 2006.
(6) Matsika, S. Conical Intersections in Molecular Systems. *Rev. Comput. Chem.* **2007**, *23*, 83−124.
(7) Moiseyev, N.; Sindelka, M.; Cederbaum, L. S. Laser-Induced Conical Intersections in Molecular Optical Lattices. *J. Phys. B: At. Mol. Phys.* **2008**, *41*, 221001−221006.
(8) Sindelka, M.; Moiseyev, N.; Cederbaum, L. S. Strong Impact of Light-Induced Conical Intersections on the Spectrum of Diatomic Molecules. *J. Phys. B: At. Mol. Phys.* **2011**, *44*, 045603−045606.
(9) Halász, G. J.; Vibók, Á.; Sindelka, M.; Moiseyev, N.; Cederbaum, L. S. Conical Intersections Induced by Light: Berry Phase and Wavepacket Dynamics. *J. Phys. B: At. Mol. Phys.* **2011**, *44*, 175102−175112.
(10) Halász, G. J.; Sindelka, M.; Moiseyev, N.; Cederbaum, L. S.; Vibók, Á. Light-Induced Conical Intersections: Topological Phase, Wave Packet Dynamics, and Molecular Alignment. *J. Phys. Chem. A* **2012**, *116*, 2636−2643.
(11) Halász, G. J.; Vibók, Á.; Sindelka, M.; Cederbaum, L. S.; Moiseyev, N. The Effect of Light-Induced Conical Intersections on the Alignment of Diatomic Molecules. *Chem. Phys.* **2012**, *399*, 146−150.
(12) Halász, G. J.; Vibók, Á.; Moiseyev, N.; Cederbaum, L. S. Light-Induced Conical Intersections for Short and Long Laser Pulses: Floquet and Rotating Wave Approximations Versus Numerical Exact Results. *J. Phys. B: At. Mol. Phys.* **2012**, *45*, 135101−135110.
(13) Kim, J.; Tao, H.; White, J. L.; Petrovic, V. S.; Martinez, T. J.; Bucksbaum, P. H. Control of 1,3-Cyclohexadiene Photoisomerization Using Light-Induced Conical Intersections. *J. Phys. Chem. A* **2012**, *116*, 2758−2763.
(14) Zavriyev, A.; Bucksbaum, P. H.; Muller, H. G; Schumacher, D. V. Ionization and Dissociation of H_2 in Intense Laser Fields at 1.064 pm, 532 nm, and 355 nm. *Phys. Rev. A* **1990**, *42*, 5500−5513.
(15) Aubanel, E. E.; Gauthier, J. M.; Bandrauk, A. D. Molecular Stabilization and Angular Distribution in Photodissociation of H_2^+ in intense laser fields. *Phys. Rev. A* **1993**, *48*, 2145−2152.
(16) Charron, E.; Giusti-Suzor, A.; Mies, F. H. Fragment Angular Distribution in One- and Two-Color Photodissociation by Strong Laser Fields. *Phys. Rev. A* **1994**, *49*, R641−R644.
(17) Giusti-Suzor, A.; Mies, F. H.; DiMauro, L. F.; Charron, E.; Yang, B. Dynamics of H_2^+ in Intense Laser Fields. *J. Phys. B: At. Mol. Phys.* **1995**, *28*, 309−339.
(18) Numico, R.; Keller, A.; Atabek, O. Laser-Induced Molecular Alignment in Dissociation Dynamics. *Phys. Rev. A* **1995**, *52*, 1298−1309.
(19) Posthumus, J. H.; Plumridge, J.; Thomas, M. K.; Codling, K.; Frasinski, L. J.; Langley, A. J.; Taday, P. F. Dynamic and Geometric Laser-Induced Alignment of Molecules in Intense Laser Fields. *J. Phys. B: At. Mol. Phys.* **1998**, *31*, L553−L562.
(20) Sandig, K.; Figger, H.; Hansch, T. V. Dissociation Dynamics of H_2^+ in Intense Laser Fields: Investigation of Photofragments from Single Vibrational Levels. *Phys. Rev. Lett.* **2000**, *85*, 4876−4879.
(21) Frasinski, L. J.; Plumridge, J.; Posthumus, J. H.; Codling, K.; Taday, P. F.; Divall, E. J.; Langley, A. J. Counterintuitive Alignment of H_2^+ in Intense Femtosecond Laser Fields. *Phys. Rev. Lett.* **2001**, *86*, 2541−2544.
(22) Serov, V. N.; Keller, A.; Atabek, O.; Billy, N. Quantitative Theory-Versus-Experiment Comparison for the Intense Laser Dissociation of H. *Phys. Rev. A* **2003**, *68*, 053401-1−053401-16.
(23) Posthumus, J. H. The Dynamics of Small Molecules in Intense Laser Fields. *Rep. Prog. Phys.* **2004**, *67*, 623−665.
(24) Serov, V. N.; Keller, A.; Atabek, O.; Figger, H.; Pavidic, D. Intense Laser Dissociation of D_2^+: From Experiment to Theory. *Phys. Rev. A* **2005**, *72*, 033413-21−.
(25) Uhlmann, M.; Kunert, T.; Schmidt, R. Molecular Alignment of Fragmenting H_2^+ and H_2 in Strong Laser Fields. *Phys. Rev. A* **2005**, *72*, 045402-5−.
(26) Wang, P. Q.; Sayler, A. M.; Carnes, K. D.; Xia, J. F.; Smith, M. A.; Esry, B. D.; Ben-Itzhak, I. Dissociation of H_2^+ in Intense Femtosecond Laser Fields Studied by Coincidence Three-Dimensional Momentum Imaging. *Phys. Rev. A* **2006**, *74*, 043411-21−.
(27) Anis, F.; Esry, B. D. Role of Nuclear Rotation in Dissociation of H_2^+ in a Short Laser Pulse. *Phys. Rev. A* **2008**, *77*, 033416-1−033416-11.
(28) Anis, F.; Cackowski, T.; Esry, B. D. Rotational Dynamics of Dissociating H_2^+ in a Short Intense Laser Pulse. *J. Phys. B: Fast Track Com.* **2009**, *42*, 091001-6.
(29) Adhikari, S.; Paul, A. K.; Mukhopadhyay, D.; Halász, G. J.; Vibók, Á.; Baer, R.; Baer, M. Photodissociation of H_2^+ upon Exposure to an Intense Pulsed Photonic Fock State. *J. Phys. Chem. A* **2009**, *113*, 7331−7337.
(30) Paul, A. K.; Adhikari, S.; Baer, M.; Baer, R. H_2^+ Photodissociation by an Intense Pulsed Photonic Fock State. *Phys. Rev. A* **2010**, *81*, 013412-1−013412-10.
(31) Calvert, C. R.; Bryan, W. A.; Newell, W. R.; Williams, I. D. Time-Resolved Studies of Ultrafast Wavepacket Dynamics in Hydrogen Molecules. *Phys. Rep.* **2010**, *491*, 1−28.
(32) Thumm, U.; Niederhausen, T.; Feuerstein, B. Time-series Analysis of Vibrational Nuclear Wave-Packet Dynamics in D. *Phys. Rev. A* **2008**, *77*, 063401-12.
(33) Fischer, M.; Grossmann, F.; Schmidt, R.; Handt, J.; Krause, S. M.; Rost, J. M. Mixed Quantum-Classical Approach to Multiphoton Dissociation of the Hydrogen Molecular Ion. *New J. Phys.* **2011**, *13*, 053019-1−053019-14.
(34) Fischer, M.; Lorenz, U.; Schmidt, B.; Schmidt, R. Fragmentation due to Centrifugal Forces in the Photodissociation of H_2^+ in Intense Laser Fields. *Phys. Rev. A* **2011**, *84*, 033422-1−033422-5.
(35) McKenna, J.; Anis, F.; Sayler, A. M.; Gaire, B.; Johnson, N. G.; Parke, E.; Carnes, K. D.; Esry, B. D.; Ben-Itzhak, I. Controlling Strong-Field Fragmentation of H_2^+ by Temporal Effects with Few-Cycle Laser Pulses. *Phys. Rev. A* **2012**, *85*, 023405-1−023405-15.
(36) He, H. X.; Lu, R. F.; Zhang, P. Y.; Han, K. L.; He, G. Z. *J.* Dissociation and Ionization Competing Processes for H_2^+ in Intense Laser Field: Which One is Larger? *Chem. Phys.* **2012**, *136*, 024311−16.
(37) Furukawa, Y.; Nabekawa, Y.; et al. Resolving Vibrational Wavepacket Dynamics of D_2^+ using Multicolor Probe Pulses. *Opt. Lett.* **2012**, *37*, 2922−2924.
(38) Handt, J.; Krause, S. M.; Rost, J. M.; Fischer, M.; Grossmann, F.; Schmidt, R. Complete Dynamics of H_2^+ in Strong Laser Fields. arXiv:1103.1565v2.
(39) Bunkin, F. V.; Tugov, I. I. Multiphoton Processes in Homopolar Diatomic Molecules. *Phys. Rev. A* **1973**, *8*, 601−612.
(40) Chu, S. I.; Laughlin, C.; Datta, K. Two-Photon Dissociation of Vibrationally Excited H_2^+. Complex Quasi-Vibrational Energy and Inhomogeneous Differential Equation Approaches. *Chem. Phys. Lett.* **1983**, *98*, 476−481.
(41) Meyer, H. D.; Manthe, U.; Cederbaum, L. S. The Multi-Configurational Time-Dependent Hartree Approach. *Chem. Phys. Lett.* **1990**, *165*, 73−78.
(42) Manthe, U.; Meyer, H. D; Cederbaum, L. S. Wave-Packet Dynamics within the Multiconfiguration Hartree Framework: General Aspects and Application to NOCl. *J. Chem. Phys.* **1992**, *97*, 3199−3213.
(43) Beck, M. H.; Jäckle, A.; Worth, G. A.; Meyer, H. D. The Multiconfiguration Time-Dependent Hartree (MCTDH) Method: A Highly Efficient Algorithm for Propagating Wavepacket. *Phys. Rep.* **2000**, *324*, 1−105.
(44) Worth, G. A.; et al. *The MCTDH package*, version 8.2 (2000); Meyer, H. D.; et al. version 8.3 (2002), version 8.4 (2007); University of Heidelberg: Germany; http://mctdh.uni-hd.de/.

(45) Meyer, H. D.; Gatti, F.; Worth, G. A. *Multidimensional Quantum Dynamics: MCTDH Theory and Applications*; Wiley-VCH: Weinheim, 2009.